

NMR Measurements Related to Clay-Dispersion Quality and Organic-Modifier Stability in Nylon-6/Clay Nanocomposites

D. L. VanderHart* and A. Asano†

Polymers Division, Mailstop 8544, National Institute of Standards and Technology, Gaithersburg, Maryland 20899

J. W. Gilman

Fire Science Division, Mailstop 8652, NIST

Received December 7, 2000

Revised Manuscript Received March 23, 2001

There is significant current interest in filled polymers, particularly using nanomaterial fillers. In this communication, we will focus on nanocomposites of nylon-6 and montmorillonite (mmt) clay.¹ Our materials have a nominal mass composition of 5% clay, and at that level, compared to the pure polymer, well-mixed (exfoliated) nanocomposites show improved mechanical properties,² improved barrier properties,³ lower water absorption,⁴ and reduced flammability.⁵

Clay is a generic name for a whole family of layered aluminosilicates,⁶ and it is rather typical of these nylon-6/clay nanocomposites that the type of clay used is a montmorillonite (mmt) clay. Such mmt clays are naturally occurring and, for the purposes of this paper, have the following characteristics:⁷ each platelike layer is about 1.0 nm thick and from 50 nm to about 100 nm in lateral dimension. The surfaces of the layer are mainly made up of silica tetrahedra while the central plane of the layer contains octahedrally coordinated Al^{3+} with frequent nonstoichiometric substitutions, where an Al^{3+} is replaced by Mg^{2+} and, somewhat less frequently, by Fe^{3+} . The concentrations of these latter ions are important for two reasons: (a) Mg^{2+} substitution leaves an embedded negative charge in the clay that must be neutralized with a cation at the surface.⁸ Usually this is an inorganic cation like Na^+ , but one can also introduce an organic cation like a tetrasubstituted ammonium ion to serve as an ionically bound organic modifier (OM). The OM is necessary for compatibilizing the nylon-6 with the clay surface. (b) Fe^{3+} is strongly paramagnetic (spin = $5/2$ in this distorted octahedral environment⁹). Typical concentrations of Fe^{3+} in naturally occurring mmt clays produce nearest-neighbor Fe–Fe distances of about 1.0–1.4 nm,¹⁰ and at such distances, the spin-exchange interaction between the unpaired electrons on different Fe atoms is expected to produce magnetic fluctuations in the vicinity of the Larmor frequencies for protons or ^{13}C nuclei.¹⁰ The spectral density of these fluctuations is important because the longitudinal relaxation, T_1^{H} , of protons (and ^{13}C nuclei) within about 1 nm of the clay surface can be directly shortened. For protons, if that mechanism¹¹ is efficient, relaxation will also propagate into the bulk of the polymer by spin diffusion.¹² Thus, this paramagnetically induced relaxation will influence the overall measured T_1^{H} to an extent that will depend both on the Fe concentration in the clay layer and, more importantly, on the average distance between clay layers. The

latter dependence suggests a potential relationship between measured T_1^{H} values and the quality of the clay dispersion since TEM images reveal that poorly dispersed clays have many unseparated layers; hence, the poorer the clay dispersion, the greater is the average distance between polymer/clay interfaces and the weaker is the average paramagnetic contribution to T_1^{H} . An important theme in this communication is to connect measured T_1^{H} 's with the quality of clay dispersion. The extent of and the homogeneity of the dispersion of the mmt layers in the nylon-6 are important for determining physical properties.¹³

There are two ways to mix nylon-6 with mmt clays, but both methods require organically modified clays (OMC). The first method is to polymerize the nylon-6 by introducing the monomer, ϵ -caprolactam, into the OMC and polymerizing, in situ. The second method involves mechanical blending of the nylon-6 polymer with OMC's.¹ The quality of clay dispersion in blending depends critically on the OM used to treat the mmt and on the processing and mixing conditions.

We discuss herein a subset of results obtained during an exploratory effort to use solid-state NMR for characterizing the nylon-6/clay nanocomposites. We consider two issues, namely, (a) the use of T_1^{H} as a measure of the quality of clay dispersion and (b) the stability of a particular OM under different processing conditions. These topics have immediate application to nanocomposite blend processing. However, we believe the arguments employed are novel, and the methods have a wider application, especially to other nanocomposite materials that have paramagnetic character. We are preparing for publication a more complete account of this research, and there will be a few references to data that we have in hand but do not discuss in detail.

Experimental Section. The samples, in the form of small pellets, were obtained from Dr. D. L. Hunter at Southern Clay Products of Gonzales, TX.¹⁴ Three of these samples, NnC-1, NnC-2, and NnC-3, appeared in a study that examined the role of mixer geometry (various twin screw designs) and shear intensity in producing the dispersion of clay in the nanocomposite.¹³ These materials all have the same overall composition and the same OMC (mmt clay treated with dimethyl dihydrogenated-tallow quaternary ammonium chloride at 1.25 equiv/kg of clay). These samples were selected on the basis of mechanical property variations as well as X-ray diffraction (XRD) and transmission electron microscopy (TEM) results that showed substantial differences in clay dispersion.¹³ The fourth sample, NnC-4, differs only in the choice of OMC (mmt clay treated with methyl, hydrogenated-tallow, bis(2-hydroxyethyl), quaternary ammonium chloride at 0.95 equiv/kg of clay); the unmodified clay is the same as for the other nanocomposites. (Hydrogenated tallow refers to a saturated, linear aliphatic substituent, of animal origin, with an even-number carbon length that can vary from 12 to 18, the average being ca. 17 carbons.) The fifth sample, N6, is that of the pure nylon-6, Capron B135WP, made by Allied Signal; this nylon was also used in the blends. Samples for NMR analysis were all vacuum-dried at 130 °C for at least 1 day; samples were either used "as-received" in pellet form or "slowly cooled" (SC). In the latter process, compacted samples were melted

† Present address: Department of Chemistry, National Defense Academy, 1-10-20 Hashirimizu, Yokosuka 239-8686, Japan

Table 1. Measured 300 MHz T_1^H , Deduced $T_{1\text{para}}^H$ Values, and Reported¹³ Properties and Processing Conditions for Samples Slowly Cooled at 1 °C/min^a

sample	NnC-1-SC	NnC-2-SC	NnC-3-SC	NnC-4-SC	N6
T_1^H (s)	0.94(3)	0.88(3)	0.60(2)	0.70(3)	1.63(5)
$T_{1\text{para}}^H$ (s) ^b	2.2(1)	1.9(1)	0.95(5)	1.37(8)	N/A
shear intensity in mixing ^c	high	high	medium	—	N/A
extruder residence time (s)	117	136	162	—	N/A
tensile yield strength (MPa)	69	80	85	—	64
% elongation (5 cm/min)	50	60	17	—	40
organic modifier ^d	M ₂ T ₂ AI	M ₂ T ₂ AI	M ₂ T ₂ AI	MT(HE) ₂ AI	N/A
TEM platelet count ^e	10	20	27	—	N/A

^a No error estimates were reported in this reference; standard uncertainties are given in parentheses for the measurements we report. N/A means "not applicable" and "—" indicates that data are unavailable. ^b This paramagnetic contribution to T_1^H is deduced using eq 1. ^c Extruders were Leistritz 34 mm modular counter-rotating twin-screw designs—intermeshing for sample NnC-1-SC and nonintermeshing for NnC-2-SC and NnC-3-SC. ^d MT(HE)₂AI = methyl, hydrogenated-tallow, bis(2-hydroxyethyl), quaternary ammonium ion; M₂T₂AI = dimethyl, dihydrogenated-tallow quaternary ammonium ion. ^e This reported platelet count represents the number of separated clay objects (multiple, unseparated layers are also counted as a single object) in a TEM image corresponding to a square region 200 nm on a side; 12 such subregions from a larger image were averaged to determine this value.

in glass tubes under N₂ at 248 °C after which they were cooled at 1 °C/min. SC samples were machined into 3 mm o.d. cylinders.

Solid-state ¹³C NMR spectra were acquired on a Bruker Avance 300 spectrometer. ¹³C CPMAS¹⁵ spectra at 75 MHz were obtained using 70 kHz decoupling fields, a 5 kHz magic angle spinning (MAS) frequency, a 1 ms cross-polarization (CP) time, and recycle delays that exceeded 5 T_1^H . Samples were thoroughly dried at 130 °C in a vacuum before NMR analysis. ¹³C signals originating from the crystalline (CR) and the noncrystalline (NC) regions of nylon-6 were separated by the method¹⁶ of spectral subtraction of signals taken at two spin-locking times, a method based on the different intrinsic $T_{1\rho}^H$ s associated with each region.

Proton spectra at 300 MHz were obtained using a low-proton-background probe manufactured by Doty Scientific of Columbia, SC. Magic angle spinning (MAS) frequencies used were 0 and 5 kHz. Bloch-decay spectra were obtained using a 90° pulse width of 1.5 μs and a 2 μs dead time. T_1^H s were measured via the inversion-recovery method using either direct proton observation or indirect ¹³C observation via CP.

All uncertainties given in this paper are standard uncertainties.

Results. Figure 1 shows ¹³C CPMAS spectra of the CR region of NnC-4-SC (representative of all of the nanocomposite spectra) and of both the CR and NC regions of N6-SC. There is a strong contrast in the line width of the CR and NC signals of N6-SC where the superior order and rigidity of the CR lattice results in sharper lines. Also, the CR signals for N6-SC and NnC-4-SC are very different and correspond to the published spectra of the α- and γ-crystalline forms.^{17,18} It is well established that the presence of the clay promotes the γ-form,¹⁹ in contrast to the formation of exclusively α-crystals in N6 for the conditions we used.

Table 1 shows the 300 MHz T_1^H s measured for each of the dried, SC samples. Also given is the paramagnetic contribution, $T_{1\text{para}}^H$, which we define in the formula

$$(T_{1\text{para}}^H)^{-1} = (T_1^H)^{-1} - [(T_1^H)^{-1}_{\text{N6}}] \quad (1)$$

where $[(T_1^H)^{-1}_{\text{N6}}]$ is the inverse of T_1^H for the N6. Equation 1 is a sum-of-rates approximation. The usual mechanism for T_1^H for N6 is spin-diffusion-distributed relaxation originating from the NC regions. (Strongly contrasting ¹³C longitudinal relaxation times for CR vs NC carbons verify this mechanism.) $T_{1\text{para}}^H$ is dependent on spin diffusion through the bulk polymer lying

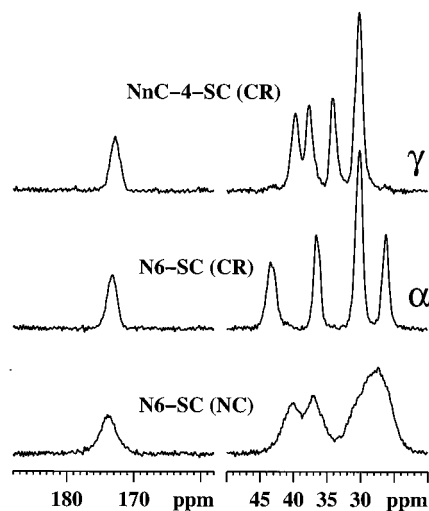


Figure 1. Deconvoluted 75 MHz ¹³C CPMAS spectra of nylon-6 in the samples indicated. Upper two spectra correspond to the crystalline regions only where the nanocomposite is dominated by the γ-phase whereas the pure nylon-6 exhibits the α-phase. The spectrum of the noncrystalline region is, by comparison, broad because there is less order and more mobility compared to the crystalline regions.

between clay surfaces. The clay surfaces are expected, on the basis of stoichiometry, to be separated by 40 nm or more. This distance is substantially larger than the typical domain thicknesses of 9 ± 2 nm (NC) and 6 ± 1 nm (CR), which we have independently determined to be typical of both N6-SC and these particular nanocomposites. The unequal spin-diffusion distances involved in the two foregoing contributions to T_1^H imply that eq 1 is only true in an averaged sense; the real T_1^H locally will depend on the distance from the nearest clay surface and whether a proton is in the CR or NC region. Equation 1 implicitly assumes that the presence of the clay does not notably influence the crystallinity or the T_1^H -determining molecular motions, compared to pure nylon. We have verified this claim by measuring T_1^H for a nanocomposite containing a diamagnetic clay. Finally, Table 1 gives other published parameters of interest for samples NnC-1-SC through NnC-3-SC.¹³ Note that the ranking of clay dispersion deduced from the $T_{1\text{para}}^H$ s and TEM are the same since longer $T_{1\text{para}}^H$ s imply poorer clay dispersion. At the same time, $T_{1\text{para}}^H$ results suggest that NnC-1-SC and NnC-2-SC are more similar with NnC-3-SC being most different while the TEM results would isolate NnC-1-SC as most different. Examining in detail why this is true is beyond the scope

of this communication; however, we note a couple of things. First, the NMR measurement averages over a much larger sample than is used for TEM; hence, when mixing is less than ideal, there is less question whether the sample examined is representative. Second, the physical principles that underlie the interpretation of the NMR measurements are sound within the assumptions made, including the assumption that the overall concentration of clay is fixed. When exfoliation is incomplete, questions arise about the distance scale of any inhomogeneities in clay distribution that ensue. The NMR measurements, which offer a simple correspondence between $T_{1\text{para}}^{\text{H}}$ and clay dispersion, will be less sensitive than, say, TEM to the details of the inhomogeneous distribution of clay. However, we believe that when clays are only partially exfoliated, this will seldom be an acceptable situation, and one will want a technique that samples a larger volume and simultaneously indicates poorer clay dispersion. At the same time, the shorter $T_{1\text{para}}^{\text{H}}$ s will readily identify good mixing albeit TEM will generally be necessary for establishing that $T_{1\text{para}}^{\text{H}}$ which corresponds to good mixing for any particular type of clay. Third, according to Table 1 and in defense of the thesis that sampling is an issue when mixing is not good, we note that the trend in “% elongation” data mimics the NMR results (in the sense that the NnC-3 sample is most dissimilar) while the “tensile yield strength” data more nearly parallel the TEM results. Finally, if the mechanical mixing is capable of breaking up the clay platelets into much smaller fragments, this can influence the T_1^{H} behavior. In the TEM images, we did not see any evidence of small clay fragments.

There are about six factors which can influence T_1^{H} for these nanocomposites, namely, B_0 (the static field used for the T_1^{H} measurement), the overall concentration of clay, the concentration of Fe^{3+} in the clay, absorbed water in the nylon, crystallinity of the nylon, and the quality of the clay dispersion. Hence, to use T_1^{H} to rank the quality of clay dispersion, it is most meaningful to make such comparisons on *dried* materials using the *same clay* with the *same clay/nylon stoichiometry*, the *same thermal history of crystallization*, and the *same B_0* .

The final topic relates to the stability of the OM and, in particular, $\text{M}_2\text{T}_2\text{Al}$, the ammonium ion with two methyl and two hydrogenated-tallow substituents. In Figure 2 we show ambient-temperature *proton* Bloch-decay spectra at 5 kHz MAS for the four NnC-SC samples, demonstrating the overall line shapes as well as focusing on the narrowed lines that sit on top of the broad nylon-6 resonance. These narrow resonances arise from decomposition products of the OM, and their spectra, for samples NnC-1-SC through NnC-3-SC, are consistent with variable amounts of a free methyl, dihydrogenated tallow amine, MT_2N . Resonances at 0.9 and 1.3 ppm are respectively associated with the methyl and most of the methylene protons of the tallow. The resonance at about 2.2 ppm is typical of protons on carbons attached to an amine nitrogen.²⁰ If the nitrogen were an ammonium nitrogen, these protons would be found above 3 ppm²⁰ where we see no intensity. The strength of the 2.2 ppm signal relative to the remaining signals indicates that this amine is mainly MT_2N instead of M_2TN . Other features of these resonances are the following: (a) The as-received pellets (data not shown) show narrow resonances with about the same

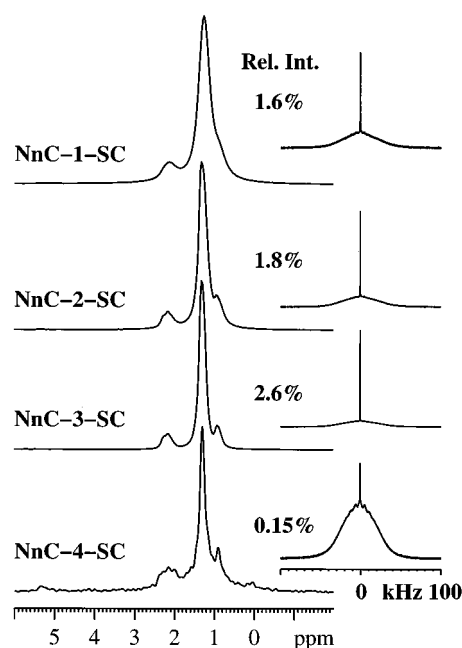


Figure 2. 300 MHz proton spectra, using 5 kHz MAS, of three identical samples (upper three spectra) whose only differences originate from different clay/polymer blending conditions (see Table 1). The lower spectrum is that of a sample having a different organic modifier (OM). On the right are the full, but differently scaled, ^1H spectra. On the left are the corresponding and horizontally expanded spectra of the very narrow components arising from the chemically degraded OM. Chemical shifts along with spectral intensities of the OM help to identify the degradation products as free amines. The overall relative intensities shown indicate that the sample with the best clay dispersion is most degraded, thereby indicating that shear stresses in blending contribute strongly to chemical degradation of the OM.

relative intensities (compared to the overall nylon-proton intensity) as their SC counterparts but have slightly poorer spectral resolution. (b) Spectra of non-spinning samples show similar narrow features (not shown) with only modestly degraded resolution; hence, the motions associated with these narrow lines arise from rapidly and nearly isotropically reorienting molecules. (c) The greatest amount of degradation is seen in sample NnC-3-SC which is judged, by $T_{1\text{para}}^{\text{H}}$ and TEM, to have the *best* clay dispersion. (d) The extent of degradation in these three samples mirrors the trend in the $T_{1\text{para}}^{\text{H}}$ data, namely, that the NnC-3-SC sample is most unique. (e) NnC-4-SC, having a pretty good clay dispersion but a different OM, shows a much weaker narrow component compared with NnC-3-SC.

From the foregoing we conclude that the degradation products are phase separated and at least 2 nm away from the surface (no significant resonance broadening¹⁰ from paramagnetic Fe^{3+}), that only minor, if any, further decomposition occurs during the temperature cycling used to prepare the SC samples, that some growth in the domain size of the decomposition products occurs in the preparation of the SC samples (slightly improved spectral resolution), and that the OM in the NnC-4 sample is chemically more stable during processing than the counterpart OM in the other three nanocomposites, provided the corresponding decomposition products in the NnC-4 sample are nonvolatile and would also phase separate.

Given that, for samples NnC-1 through NnC-3, the processing temperature for mixing was very close to that

used in melting the SC samples and that the time of exposure during the melting, prior to cooling, was vastly longer (hours) than the exposure during mixing (minutes), it would appear that at a temperature like 240 °C *the presence of the shear field in mixing is a much more important condition for producing degradation of the OM compared with temperature alone.* In fact, if we translate the relative intensity of the narrow component into a fraction of the OM that had degraded in the NnC-3-SC sample, then it looks like $83 \pm 10\%$ of the original OM is now decomposed in this way. Given that exfoliation is probably still incomplete in this sample, these results suggest that *when this OMC surface is exposed to the polymer under shear mixing, nearly all of the OM on any exposed face is degraded.* Hence, while the OM in these three nanocomposite samples seems to serve as a vehicle to promote mixing initially, its role in the final establishment of affinity between polymer and clay surface is no longer played. Certainly, however, there must be charged species left at the surface in order to maintain charge neutrality, and these charged species will play some, as yet unknown, role in establishing affinity of the polymer for the clay surface.

We have shown that NMR techniques are useful in characterizing clay dispersion and, in certain cases, for following the fate of the organic modifier during processing. In a larger future publication, we will treat these and other issues in more detail. For example, we will compare blended samples with in situ polymerized samples. Also, we will monitor the influence of annealing and will demonstrate how one can use the paramagnetism of the mmt clay to establish the relative position of α - and γ -crystallites when both coexist in a NnC structure. In principle, the use of T_1^H as a relative measure of clay dispersion can be applied to other nanocomposites containing mmt clay so long as (a) $T_{1\text{para}}^H$ is not substantially longer than the T_1^H of the pure polymer and (b) the clay does not strongly alter the morphology and dynamics of the polymer.

References and Notes

(1) Alexandre, M.; DuBois, P. *Mater. Sci. Eng.* **2000**, *28*, 1.

- (2) Kojima, Y.; Usuki, A.; Kawasumi, M.; Okada, A.; Fukushima, Y.; Kurauchi, T.; Kamigaito, O. *J. Mater. Res.* **1993**, *8*, 1185.
- (3) Messersmith, P. B.; Giannelis, E. P. *J. Polym. Sci., Part A: Polym. Chem.* **1995**, *33*, 1047.
- (4) Okada, A.; Fukushima, Y.; Kawasumi, M.; Inagaki, S.; Usuki, A.; Sugiyama, S.; Kurauchi, T.; Kamigaito, O. US Patent 4,739,007, 1988.
- (5) Gilman, J. W.; Jackson, C. L.; Morgan, A. B.; Harris, R. H.; Manias, E.; Giannelis, E. P.; Wuthenow, M.; Hilton, D.; Phillips, S. *Chem. Mater.* **2000**, *12*, 1866.
- (6) Theng, B. K. G. *Clay-Organic Reactions*; Adam Higler: London, 1974.
- (7) *The X-ray Identification and Crystal Structures of Clay Minerals*; Brindley, G. W., Ed.; The Mineralogical Society: London, 1951.
- (8) Dombrowski, T. In *Kirk-Othmer Encyclopedia of Chemical Technology*, 4th ed.; John Wiley & Sons: New York, 1993; Vol. 6, pp 381–405.
- (9) Bensimon, Y.; Deroide, B.; Zanchetta, J. V. *J. Phys. Chem. Solids* **1999**, *60*, 813.
- (10) Yang, D.-K.; Zax, D. B. *J. Chem. Phys.* **1991**, *110*, 5325.
- (11) Blumberg, W. E. *Phys. Rev.* **1960**, *119*, 79.
- (12) *The Principles of Nuclear Magnetism*; Abragam, A., Ed.; Oxford University Press: New York, 1961; Chapter V.
- (13) Dennis, H. R.; Hunter, D. L.; Chang, D.; Kim, S.; White, J. L.; Cho, J. W.; Paul, D. P. *Proceedings of ANTEC 2000*, Orlando, May 2000.
- (14) Certain commercial companies are named in order to specify adequately the experimental procedure. This is no way implies endorsement or recommendation by the authors or their agencies.
- (15) Schaefer, J.; Stejskal, E. O.; Buchdahl, R. *Macromolecules* **1977**, *10*, 384.
- (16) VanderHart, D. L.; Pérez, E. *Macromolecules* **1986**, *19*, 1902.
- (17) Okada, A.; Kawasumi, M.; Tajima, I.; Fukushima, Y.; Kurauchi, T.; Kamigaito, O. *J. Appl. Polym. Sci.* **1989**, *37*, 1363.
- (18) Hatfield, G. R.; Glans, J. H.; Hammond, W. B. *Macromolecules* **1990**, *23*, 1654.
- (19) Maxfield, M.; Christiani, R.; Murthy, S. N.; Tuller, H. US Patent 5,385,776, 1995.
- (20) *Aldrich Library of ^{13}C and ^1H FTNMR Spectra*; Pouch, C. J., Behnke, J., Eds.; Aldrich Chemical Co.: Milwaukee, WI, 1993; Vol. 1.

MA002089Z